Mößbauer Effect Lab Report

A7

Jacob Cardinal Tremblay, Pranav Limaye

September 29, 2022

K221

Contents

1 Introduction

This experiment consists of many important parts, which all contribute to the overall goal of helping introduce Master's students a scientific project involving Mößbauer spectroscopy.
The Mößbauer effect was discovered by the scientist Rudolf Mößbauer in 1958 for which he was also awarded the Nobel Prize in Physics in 1961 [1]. During this time, various researchers were trying to produce recoilless emission in order to get highly precise and resolved spectra. Techniques like physically moving the sample to compensate for the Doppler broadening took place, but with no success. It was Mößbauer who came up with the idea of using a sample with a crystal lattice in order to successfully achieve recoilless emission and absorption of γ-rays. This same idea is what will be explored in this lab by using ^{57}Co as the radioactive source and observing the hyperfine structure of the 14.4 keV transition in ^{57}Fe. This method is used in this experiment as a way to investigate line width, Lande factors, isomeric shift and much more.

2 Basics of Mößbauer Spectroscopy

This introduction to the world of Mößbauer Spectroscopy is our very own summary and interpretation of the topics mentioned in literature included in the 2022 lab script [6], along with other sources which are cited. Please view the information in this report as a concise version of the material, focused around the specific tasks performed. For a full understanding, please seek information from our cited sources.

2.1 Resonance Absorption and Natural Line Width

A γ-ray may only be absorbed if it has an energy equal to the excitation energy of the nucleus of the absorbing atom. The emission of a γ-ray will not necessarily have a resulting energy equal to the transition energy since the emitting nucleus will recoil and therefore the γ-ray will have an energy smaller than the nuclear transition energy. One may also observe a similar effect during absorption, where part of the *gamma*-ray energy will be converted to kinetic energy due to conservation of momentum. This energy loss, however, can be avoided if both the emitting and absorbing nuclei are part of a crystalline solid [9]. This is because the mass of the crystal is much larger than the single atom and therefore the energy loss due to recoil will be absorbed by the crystal and will be negligible. The Mößbauer effect is defined as this recoil-less emission and absorption of γ-radiation.
The frequency spectrum of emitted γ-rays have a Lorentz distribution (described in Fig. 1) which has a half-width of $\Gamma/\hbar$ centered at ω_0,

$$I(\omega) = \frac{I_0}{1 + \left[(\omega - \omega_0)\, 2\hbar/\Gamma\right]^2} \tag{1}$$

where $I(\omega)$ is the intensity of radiation at a frequency of ω. Γ represents the natural line width and is the energy uncertainty of a nuclear level, $\Gamma = \hbar/\tau_{\mathrm{N}}$, with mean lifetime given by τ_{N}.
For ^{57}Fe, the energy transition is of 14.4 keV and there is a lifetime of 1.41×10^{-7} s, which gives a linewidth of,

$$\Gamma = \hbar/\tau_{\mathrm{N}} = 4.7 \times 10^{-9} eV \tag{2}$$

and a relative energy uncertainty of,

$$\Gamma/\hbar\omega_0 = 3.3 \times 10^{-13}. \tag{3}$$

By measuring the resonant absorption, it is then possible to observe the energies with a precision which is limited by the natural linewidth [9].

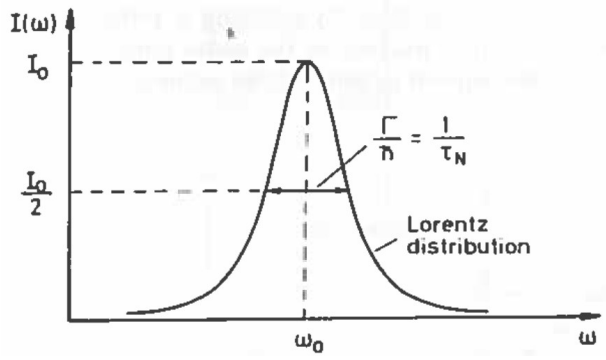

Figure 1: The intensity distribution for emitted γ-radiation from nuclear decay. Source: [9].

2.2 Doppler Broadening and Recoil Energies

If we consider a monoatomic gas in thermal equilibrium, the recoil and reduction in energy during the emission (or absorption) of γ-rays will have an impact on their frequency spectrum. The frequency spectrum will have shift in ω_0 by the recoil energy and the line will be broadened due to the Maxwell velocity distribution of the atoms. Because a gas is not embedded into a crystal lattice, an atom which is emitting a γ-ray will experience some recoil. This recoil requires energy, and therefore the emitted *gamma*-ray will be at a lower energy. Because the γ-ray is now at a lower energy, it no longer has the same energy as between the excited state and ground state and is therefore unable to excite the other atom. This difference in energy, before and after emission can be described by,

$$E_{\text{before}} - E_{\text{after}} = \hbar\omega = \hbar\omega_0 + \hbar\,(k \cdot \nu) - \frac{\hbar^2 k^2}{2\text{M}}. \tag{4}$$

This recoil effect is also present during absorption due to the momentum which is imparted on the nucleus. The atom will experience recoil when a γ-ray is absorbed which also causes the *gamma*-ray to be of lower energy, and therefore the nucleus is unable to be excited.

Because of this recoil effect, the emission peaks of the spectral line will be shifted to

a lower frequency whereas any absorption peaks will be shifted to a higher frequency. In such a gas, any resonant absorption would be very small because only the wings of emission and absorption overlap. Since the absorption takes place over a large frequency range, this process is also not very selective. A characterizing feature of the Mößbauer effect is that most of the emission and absorption spectrum is located in a small region around ω_0.

The solution to eliminating the recoil is to use emitting and absorbing nuclei which are in a crystal lattice. The binding energy is much larger than the recoil energy and therefore any recoil energy will be absorbed by the lattice and eliminate any recoil. Because the mass of the lattice is much larger than the mass of a single atom, the change in energy of a single atom in the lattice is negligible.

The $\hbar\,(k \cdot \nu)$ term in Eqn. 4, refers to the velocity dependant Doppler effect. This effect arises from the fact that any emitted γ-ray will have a lower or higher energy depending on if the emitting atom is moving away or towards to absorbing atom. This effect can also be relevant if the absorbing atom is in motion or if both atoms are in motion. This change in velocity could change the frequency of the *gamma*-waves and therefore allow them to be absorbed more often or less often depending on how close the γ-ray's energy is to the energy between the ground state and excited state of the absorbing atom. The closer the energies are to each other, the more *gamma*-rays will be absorbed, and therefore the less the detector will observe. This means that the larger the dip observed by the detector, the more that the energies will be overlapping, with a minima occurring at resonance. This concept is described in Fig. 2.

2.3 Debye-Waller Factor

If an atom is in a relatively massive solid and the vibrational motion of an atom is not significantly altered following the emission of a γ-ray, then one will obtain an unbroadened and unshifted Mößbauer line. The Debye-Waller factor is the ratio of this unshifted γ-ray emission to the total emission and is denoted by f. The Debye-

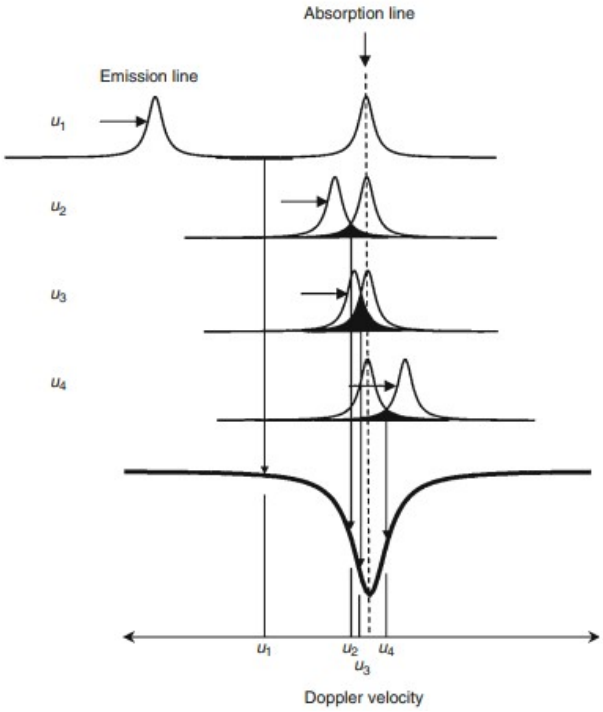

Figure 2: A schematic representing the concept of Doppler shift in Mößbauer Spectroscopy. Source: [12].

Waller factor is essentially describing how the atomic motion in the solid attenuate the central unshifted Mößbauer line and adds side bands. This factor is temperature dependant and will be at its largest at $T = 0$, however it will always be smaller than 1 due to zero-point energy. We can classically describe the Debye-Waller factor as depending on the mean square displacement of the atom,

$$f = \exp\left(\frac{k^2 \langle u^2 \rangle}{3}\right) \tag{5}$$

where $\langle u^2 \rangle = 3 \langle x^2 \rangle$. If we are considering more than a single phonon frequency, then Eq. 5 cannot be used. In such a case we need to consider a the phonon density of states $Z(\Omega)$ and our factor becomes,

$$f(T) = \exp\left\{-\frac{\hbar k^2}{6MN} \int_0^\infty \frac{Z(\Omega)}{\Omega} \left[1 + \frac{2}{\exp(\hbar\Omega/k_\mathrm{B}T) - 1}\right] \mathrm{d}\Omega\right\}. \tag{6}$$

The Debye model can be a good approximation for a realistic case. In such a model, the phonon density of states is given by,

$$Z(\Omega) = \frac{9N\hbar^3\Omega^2}{h_{\mathrm{B}}^3\Theta^3} \quad \text{for } \Omega \leq \Omega_{\mathrm{D}}. \tag{7}$$

If $\Omega > \Omega_{\mathrm{D}}$ then $Z(\Omega) = 0$ and $\Omega_{\mathrm{D}} = k_{\mathrm{B}}\Theta/\hbar$ is the Debye frequency and Θ is the Debye temperature. If the temperature is greater than the Debye temperature, then $\langle x^2 \rangle$ will increase linearly with temperature, but if it is smaller than the Debye temperature, $\langle x^2 \rangle$ will increase according to T^2.
For this experiment, the temperature will lie below the Debye temperature and therefore will have a resulting Debye-Waller factor of the form,

$$f_{\mathrm{D}}(T) = \exp\left\{-\frac{\hbar^2k^2}{2M}\frac{3}{2k_{\mathrm{B}}\Theta}\left[1 + \frac{2\pi^2}{3}\left(\frac{T}{\Theta}\right)^2\right]\right\}. \tag{8}$$

From Eqn. 8, we can understand a few important relationships:

- By measuring the Debye-Waller factor, information about the phonon frequency spectrum can be obtained.
- Increasing the recoil energy will cause a decrease in the Debye-Waller factor. If there is to be a measurable Mößbauer effect, then E_γ cannot be too large since $hk = E_\gamma/c$. Generally, the values for E_γ are smaller than 100 keV [9].
- For an ideal observation of a large Mößbauer effect, low temperatures ($T < \Theta$) are better. The maximum Debye-Waller factor is at $T = 0$, however even at such low temperatures f_{D} will be smaller than 1 because of the zero point energy which describes that a quantum mechanical system will have a finite energy even at $T = 0$.

2.4 Mößbauer Sources

There are many sources which may be used as Mößbauer sources, however they must fulfill some conditions:

- The observed γ-ray must lead to the ground state because absorption may only happen from the ground state of a stable isotope.
- The Debye-Waller factor cannot be too small, it is important that the temperatures are low, γ-ray energy should be low, Debye temperature should be high and the atomic mass must be large.
- In order for the linewidth not to be too small, it is important that the lifetime of the Mößbauer level is not too short. Otherwise, the energy resolution could also be too poor.
- The parent isotope must be practical to handle and use in the experimental laboratory. This means that its properties in relation to the lab conditions as well as ease of production must be considered.

There are several Mößbauer sources which one can consider, such as $^{67}Ga -^{67} Zn$, $^{119}Sn - isomer$, $^{151}Sm -^{151} Eu$, more details on each source can be found in [9], however in our experiment we will be using $^{57}Co -^{57} Fe$. The ^{57}Co isotope is produced in the nuclear reaction ^{56}Fe(d,n)^{57}Co and the decay of ^{57}Co mostly occurs due to electron capture from the K shell. This K shell will then be filled by a higher shell which gives an emission of 6.4 keV in the X-ray, while the transition from the Mößbauer level to the ground level releases 14.4 keV. The decay scheme is shown in Fig. 3.

There are certain advantages to using ^{57}Co-^{57}Fe. This includes that the parent isotope (^{57}Co) has a long half-life of $t_{1/2} = 270$ days, which means that many experiments may be performed before needing to change sources. The lifetime of the Mößbauer level is of $t_{1/2} = 98$ ns, which gives a linewidth with good energy resolution and does not require extreme experimental procedures. The 14.4 keV energy is also small, which therefore allows for room temperature measurements even with relatively large Debye-Waller factors. A small drawback of using this source however is that small γ-ray energies could make it hard to discriminate γ-rays from the emitted X-rays [9].

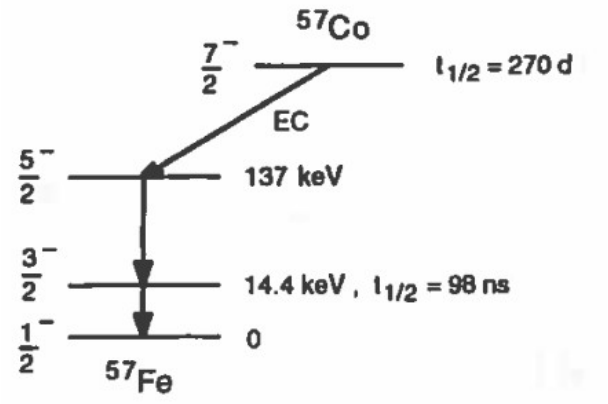

Figure 3: Decay scheme of ^{57}Co to ^{57}Fe. Source: [9].

2.5 Hyperfine Structure

Hyperfine structure refers to the splitting of spectral lines into components. These splittings happen due to nuclear effects an must be observed through a spectroscope with the aid of an interferometer [5]. In our case, this is important as hyperfine structures will arise throughout Mößbauer spectroscopy, therefore we discuss the main hyperfine interactions in this section.

2.5.1 Isomeric Shift

The isomer shift happens because of when an electron is orbiting a nucleus at a certain radius, the energy of a nucleus is shifted relative to a point nucleus. In the experiment, the difference in the monopole energies is what causes a shift in the resonance. The energy shift in the ground state might differ from the excited state, which is what we observe in Mößbauer spectroscopy. However, we only observe the difference between the ground state and the excited state and not any particular shift in levels.
This shift will be positive if the radius in the excited state is larger than the ground

state, and negative in the opposite situation. In our case, ^{57}Fe has a smaller radius in the excited state compared to in the ground state and therefore the shift is negative.

2.5.2 Electric Quadrupole Interaction

The electric quadrupole interaction occurs when a non-spherical nucleus interacts with an electric field gradient. The energy levels will split since the degeneracy of the M sublevels is lifted. For ^{57}Fe, the electric quadrupole splitting is shown in Fig. 4.

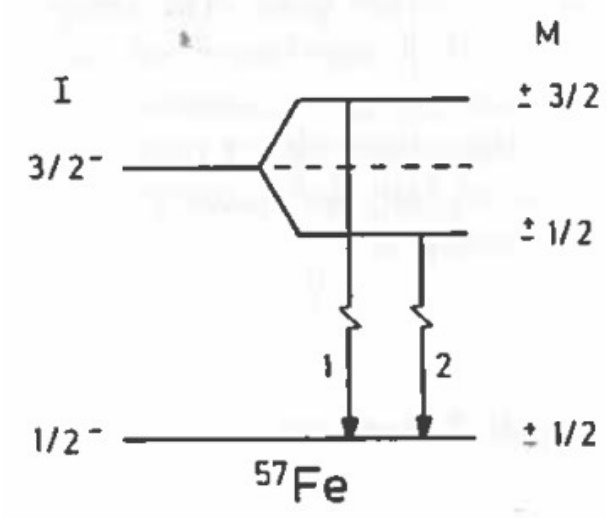

Figure 4: Quadrupole splitting of the ^{57}Fe Mößbauer transition. Source: [9].

2.5.3 Magnetic Dipole

The magnetic interaction $-\boldsymbol{\mu} \cdot \mathbf{B}$ causes a nuclear level splitting that has equal separation between magnetic sublevels, which then causes a splitting in the energy of the emitted γ-rays. We can see this magnetic splitting for the case of ^{57}Fe in Fig 5. The internal magnetic fields of the iron isotope will split the I = 3/2 level into

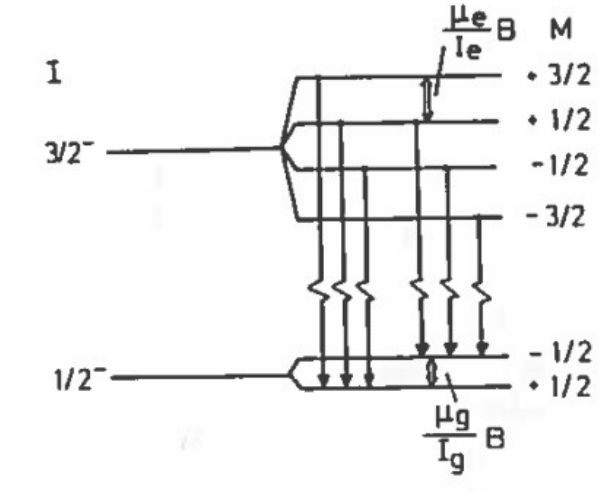

Figure 5: The splitting of the nuclear sublevels of ^{57}Fe in a magnetic field. Source: [9].

4 separate sublevels and the I = 1/2 level into two other sublevels. Because of the selection rules for transitions which state that $\delta_I = 0, \pm 1$, there are only 6 possible transitions, which results in six dips in the spectrum. We may also note that the distance between the furthest dips are proportional to the internal magnetic field, and the intensities of each dip are not equal, but depend on the direction and strength of the external field.

3 Experimental Setup

In this experiment, ^{57}Co was used as a radioactive decay element to observe the recoilless emission and absorption of γ-rays. This is done by having the emitter shielded into a lead box with a small opening for the γ-rays to transmit and have it fixed in place whereas the absorber is moving away and towards the emitter. Due to this relative velocity, the emission/absorption lines will be redshifted or blueshifted. The emission which is the result of ^{57}Fe excited state transition to the ground level

occurs at an energy of 14.4 keV and hence the resonant nuclear absorption by the target is observed within the frequency range equivalent to 14.4 keV with a Single Channel Analyzer (SCA).
Our experiment is set up in transmission geometry, where the detector is placed behind the absorber and therefore measures the photons which are transmitted through the absorber. Such a detector must be able to measure ionising radiation such as an ionisation chamber or scintillation detector.
The experimental setup block diagram can be seen in Fig. 6.

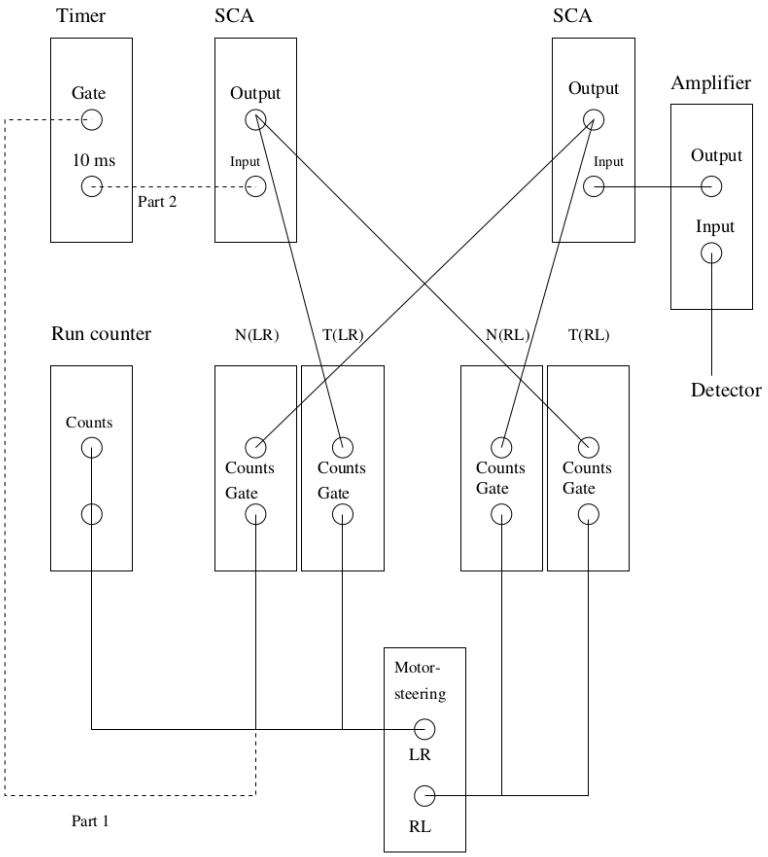

Figure 6: Circuit layout of the experimental setup. Source: [6].

3.1 Observing the γ-ray Emission Spectra

First, the γ-ray emission spectrum was obtained on the channel analyzer by setting the counter gets open for 10 seconds. Within the SCA, the voltage window interval was 50 ± 1 mV and the voltage was varied through steps of 20 ± 2 mV starting from 300 ± 2 mV all the way up to 4200 ± 2 mV. Where the largest uncertainties are due to potential human error in aligning the voltage dials. These values were chosen as this is a range in which the Mößbauer peak should be visible. The different potentials refer to different energy levels of the emission spectra.
Plotting the data for total photon counts per second as a function of voltage thus gave three distinct emission lines. The first line being the 6.4 keV transition of Fe due to the K-shell filling, second line is the desired Mößbauer spectra and the third line is a superposition of these two lines respectively. In Fig. 7 a significant low voltage background can be seen caused by free electrons in the setup which give a pseudo photon count and can be accounted as pure electron noise signal. In this background one might claim to detect a small peak, however, this is most likely just an artifact of the noise and low sampling of this part of the graph and not actually physical.

3.2 Mößbauer Spectroscopy

By using the 14.4 keV line of ^{57}Fe observed in the above section, it is then possible to study the hyperfine interactions using Mößbauer spectroscopy. In order to perform Mößbauer spectroscopy, the upper and lower voltage bounds need to be known so that the Mößbauer spectrum is visible. Using Fig. 7, it was determined that SCA1 had to set to $V_{low} = [2200 \pm 1.0]$ mV and $V_{high} = [3000 \pm 1.0]$ mV and therefore $\Delta V = [800 \pm 1.4]$ mV.
Another important factor in Mößbauer spectroscopy is that either the source or the absorber has to be moving. In this experiment, the Fe absorber moves towards and

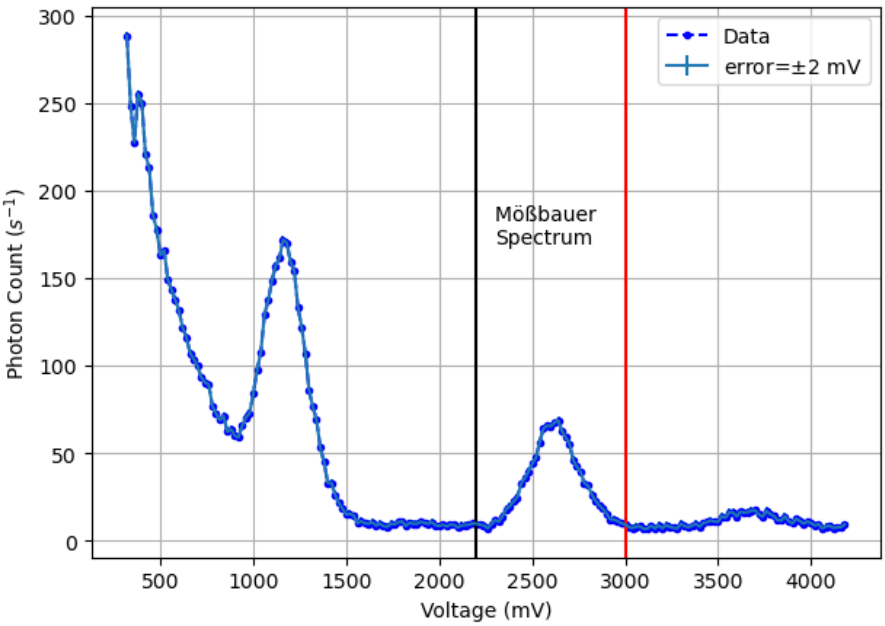

Figure 7: Emission Spectra from radioactive decay of ^{57}Co. Previously discussed uncertainties of ±2 mV are added on each point however, they are very small therefore hard to visualize on the graph.

away from the source at a constant velocity. The velocity starts at a higher value (in this case 6.6 mm/s) and is gradually lowered to the lowest velocity (in this case 0.2 mm/s). This lower velocity was chosen as any velocity much lower than this would not only take extremely long to carry out, but problems due to friction could arise, where the target could get "stuck" and therefore might not actually move at the speed with which it is assumed to be moving. Nonetheless, 0.2 mm/s is a low enough velocity to resolve the Mößbauer spectrum.

As by convention, the movement from left to right is taken as a positive velocity, whereas the movement from right to left is taken as a negative velocity. As the target moves towards the source (right to left), the counter gate N(RL) and the time gate T(RL) are set to open. The opposite is true as the target moves away from the source as N(LR) and T(LR) are set to open. This resulted in a total spectrum which

was taken in the velocity ranges between -6.2 mm/s and 6.6 mm/s. The absorber may complete multiple passes moving back and forth until the person controlling the experiment decides to stop the experiment after a certain number of passes. The number of passes is noted for every measurement because as the velocities start to decrease, the more it takes time to complete passes and the less reasonable it becomes to measure multiple passes. For this reason the measurements at lower velocities are taken with a lower number of passes.
The values for velocity were determined using,

$$v_{\mathrm{RL}} = \frac{D \cdot P}{t_{\mathrm{RL}}}, \qquad v_{\mathrm{LR}} = \frac{D \cdot P}{t_{\mathrm{LR}}}, \tag{9}$$

where D is the distance travelled by the absorber and is $D = 25.1 \pm 0.02$ mm. P is the number of passes, and t is the time taken to complete the number of passes.

4 Analysis and Results

4.1 Debye-Waller Factor

The Debye-Waller Factor was calculated using,

$$f_{\mathrm{D}}(T) = \exp\left(\frac{-\hbar^2 k^2}{2M}\frac{3}{2k_{\mathrm{B}}\theta}\left[1 + \frac{2\pi^2}{3}(\frac{T}{\theta})^2\right]\right). \tag{10}$$

where for ^{57}Fe, the recoil energy term, (i.e, $-\frac{\hbar^2 k^2}{2M}$) is equal to 2×10^{-3} eV, and the Debye temperature is $\theta \approx 470$ K. The average room temperature throughout the experiment was around $T = 288 \pm 1$ K. One might notice that this temperature appears somewhat cold for room temperature, however the windows were open, which let the cool air from outdoors into the experiment room.

Hence, taking into account these values for ^{57}Fe and the constants, the Debye-Waller Factor calculated for the experiment was,

$$f_{\mathrm{D}}(T) \approx 0.773 \pm 0.007 \tag{11}$$

The ideal Debye-Waller factor for ^{57}Fe should be 1 [9]. Therefore, the experiment was relatively close to the perfect factor considering it was performed at room temperature, as a percent error of 22.7% was obtained.

4.2 Mößbauer Spectroscopy and Curve Fit

As can be seen in Fig. 8, there were 6 separate absorption peaks which were detected, which show the Mößbauer hyperfine spectrum. The y-axis shows the detected number of counts per second, which have been normalized by the maximum value. One may notice that the error bars are lower as we approach zero. Statistically speaking, the more counts received for a particular velocity, the more the random uncertainty will be minimized. This means that since the lower velocities receive a higher number of counts than the higher velocities, we are able to consider smaller uncertainties. These uncertainties were calculated according to Eq. 21 in the appendix.

The velocities were then converted into energies for further analysis, using,

$$\Delta E = \frac{14.4 \text{ keV} \cdot v \text{ [mm/s]}}{c \text{ [mm/s]}} \tag{12}$$

Where v is the velocity and c in the speed of light. The resulting energy values were then converted to neV to simplify calculations. The curve fit was done using the `Python` programming language [11] and the `scipy.optimize.curve_fit` package [4]. Here we first created individual Lorentzian curve fits to each separate peak of the form,

$$f(\tau, \nu) = a \cdot \frac{(\tau/2)^2}{(\nu - \nu_0)^2} + b. \tag{13}$$

These individual curves were then added together to create the fit seen in Fig. 8. The `Scipy` software then provided us with the fit parameters which are listed in Tab. 1.

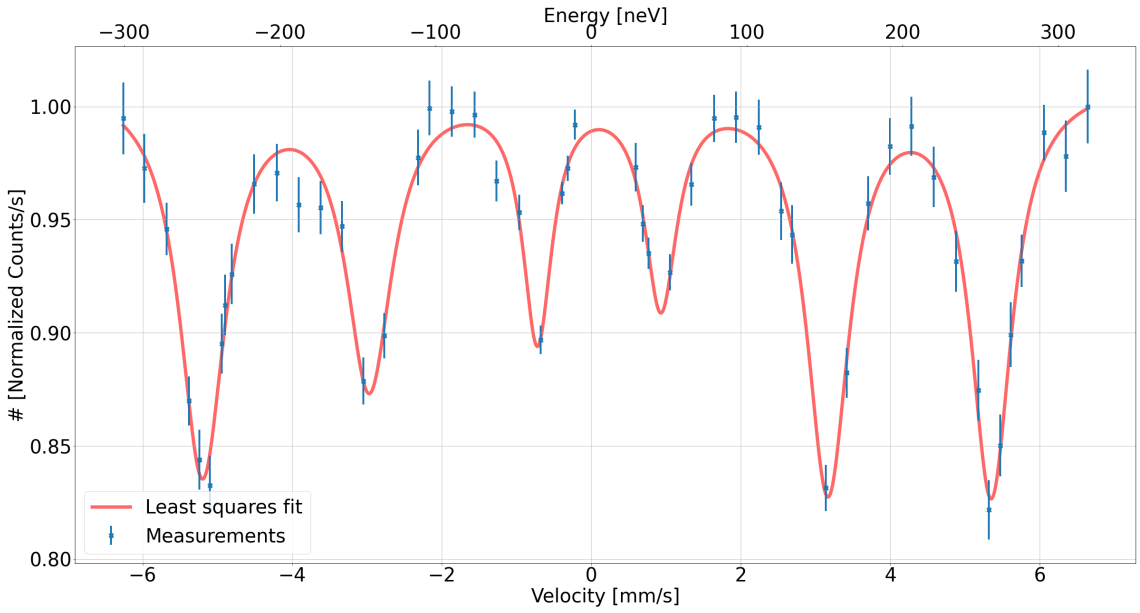

Figure 8: Cumulative Lorentz peak curve fit applied to the measured 14.4 keV Mößbauer hyperfine spectrum.

Peak	Center [neV]	Width [neV]	Amplitude [s^{-1}]
1	-249.78 ± 0.85	35.59 ± 3.36	-0.17 ± 0.009
2	-142.62 ± 1.47	35.96 ± 5.35	-0.13 ± 0.011
3	-34.59 ± 1.61	23.09 ± 3.78	-0.11 ± 0.012
4	44.75 ± 1.40	25.37 ± 7.50	-0.095 ± 0.017
5	152.09 ± 1.28	33.27 ± 3.42	-0.18 ± 0.011
6	256.98 ± 0.80	32.05 ± 3.21	-0.18 ± 0.009

Table 1: Parameters for the curve fit to the Mößbauer spectrum. Peaks are ordered from left to right according to Fig. 8.

4.3 Line Widths

We can see from Tab. 1 that the measured line widths vary between 36.96 ± 5.35 neV and 23.09 ± 3.78 neV. The natural line width is equal to half these values which means

between 18.48 ± 2.675 neV and 11.545 ± 1.89 neV. The accepted value of the natural line width for ^{57}Fe is of 4.7 neV [13], however, because we are observing absorption lines where the transition for emission and absorption is the same, these lines will be a convolution of the emission and absorption line of ^{57}Fe [10]. This then means that the lines we observe should have a natural linewidth of 9.4 neV. Comparing our values in Tab. 1 or to our mean line width (30.89 ± 1.92 neV) we can see that they are larger than the theoretical value. This however is most likely due to the fact that our Debye-Waller factor us less than 1 which causes the line to be broader than the natural line width. It is also possible that this line-broadening be due to some thermal Doppler broadening where the recoilless absorption was not perfect. We may also notice that the line widths are larger for peaks where the velocity of the absorber was higher. This could be due to impurities in the crystalline structure of the absorber. This would mean that the electric field gradient could undergo local changes and therefore local quadrupole shifts would increase the linewidth. This broadening could also happen when an unresolved quadrupole shift is present [2; 3].

4.4 Lande Factors

The g-factor or Lande factor can be determined using the equation,

$$\Delta E_{\mathrm{I}} = -g_{\mathrm{I}} \mu_{\mathrm{N}} B. \tag{14}$$

Therefore it is then possible to calculate the Lande factors for both the ground and excited states. Here we assume a magnetic field value of $H = 333 \pm 10$ kG which was given in the lab script [6], and a nuclear magneton value for iron of $\mu_{\mathrm{N}} = 3.15 \cdot 10^{-12}$ eV/Gauss [7].

We start by finding the Lande factor for the ground state. This means that we take the energy difference between the 2 and 4 transitions and the 3 and 5 transitions. We can then take the energy difference between the excited states of 1 and 2, 2 and 3, 4 and 5, and 5 and 6. It is then trivial to calculate the Lande factor from Eq. 14

which rearranges into Eq. 15,

$$g_{\mathrm{I}} = \pm \frac{\Delta E_{\mathrm{m}}}{\mu_{\mathrm{N}} B}. \tag{15}$$

The values of these energy differences and the Lande factors are shown in Tab. 2.

space	Transition	ΔE [neV]	g_I [ ]
g_e	Δ_{12}	104.90 ± 1.51	-0.100 ± 0.0033
g_e	Δ_{23}	107.34 ± 1.89	-0.102 ± 0.0035
g_e	Δ_{45}	108.04 ± 2.18	-0.103 ± 0.0037
g_e	Δ_{56}	107.16 ± 1.70	-0.102 ± 0.0035
g_g	Δ_{24}	186.67 ± 2.06	0.178 ± 0.0057
g_g	Δ_{35}	187.37 ± 2.03	0.179 ± 0.0057

Table 2: Energy differences and Lande factors of excited and ground state (g_e, g_g).

From Tab. 2, we can then identify that the average energy for the ground state is $\Delta E_{1/2} = -187.02 \pm 1.44$, and therefore the Lande factor is $g_{1/2} = 0.178 \pm 0.006$. Similarly, the average energy for the excited state is $\Delta E_{3/2} = 106.86 \pm 0.61$ and therefore the Lande factor is $g_{3/2} = -0.102 \pm 0.003$. We can compare our obtained values for the Lande factor to the theoretical values by taking the ratio of the two Lande factors. The ratio for theoretical values is $g_{1/2}/g_{3/2} = -1.752 \pm 0.004$ [8]. The ratio of the experimentally determined Lande factors is $g_{1/2}/g_{3/2} = -1.750 \pm 0.077$, therefore the obtained error is 0.00103 ± 0.0442 or $[0.103 \pm 4.42]\,\%$. Such a low error allows us to make a confident claim that our experimental values agree with the theoretical values, and that the values obtained are reasonable for this type of experiment.

4.5 Quadrupole Splitting

In the previous *Line-Width* section, we quickly discuss that line broadening could be the result of quadrupole splitting. Here we can take a look at that claim and

determine if quadrupole splitting made a significant contribution. It is expected that quadrupole interaction would remove the degeneracy between the $|m| = 1/2$ and the $|m| = 3/2$ levels. For significant quadrupole splitting, we would expect that the shift be positive for $|m| = 3/2$ states and negative for $|m| = 1/2$ states. If we look at our results in Tab. 2, we see that Lande factors for the excited states as well as the ground states are relatively similar. This gives us an ideas that any quadrupole shift is most likely negligible or else we would see significantly different values in the energy difference of the excited state. We can further test this by calculating the energy difference due to quadrupole splitting,

$$\frac{\Delta E_{56} - \Delta E_{12}}{2} = [1.13 \pm 1.13] \text{ neV}. \tag{16}$$

This shows us that the energy difference due to quadrupole splitting is close to zero and is many orders of magnitude lower than hyperfine splitting. We also see that since the uncertainty is just as large as our obtained value, we can consider a value of zero within the error. Comparing our results to the theory, we conclude that our electric quadrupole shift measurement is very small and even consistent with zero, and therefore the effects due to quadrupole splitting are negligible.

4.6 Isomeric Shift

If we were to overlay the negative peaks and the positive peaks when taken as absolute values, one would see that they are not perfectly symmetric. This is due to the isomeric shift which shifts the entire spectrum by ΔE_{iso}, due to electric monopole interaction. If the peaks were symmetric, the average center of a negative peak and it's respective "equivalent but opposite" positive peak would be zero. Since all the peaks have a corresponding peak of negative value, if there were no shift, we would expect the average center value of all the peaks to be equal to zero. Using the center peaks shown in Tab. 1, we therefore calculate the isomeric shift to be,

$$\Delta E_{iso} = [4.471 \pm 0.519] \text{ neV}. \tag{17}$$

We therefore see that we do in fact have an isomeric shift (although it is small) since our result is not equal to zero. This shift is most likely due to the material in which the ^{57}Co and ^{57}Fe are contained which add small contamination. Unfortunately we cannot compare our obtained value to the literature as this value will depend on electron densities and therefore the specific composition of the source and absorber as well as the temperature. These reasons are also important to why our obtained value is not equal to zero. Note that we observe a positive shift, however, theory predicts that we should observe a negative shift for ^{57}Fe (see section 2.5.1 for more details). The positive result is not a problem however as this only depends on how the velocity directions are defined. Therefore it is possible to obtain either a positive or negative result, and in our case, if we had defined our velocities opposite as what they are now, we would have obtained a value of $\Delta \mathrm{E}_{\mathrm{iso}} = [-4.471 \pm 0.519]$ neV.

5 Conclusion

The aim of this laboratory experiment was to record and analyse the 14.4 keV Mößbauer spectrum of ^{57}Fe. A γ-ray emission spectrum was first recorded and the Mößbauer peak was identified between $\mathrm{V}_{low} = [2200 \pm 1.0]$ mV and $\mathrm{V}_{high} = [3000 \pm 1.0]$ mV. This spectrum was then measured at a higher resolution where the hyperfine structure was identifiable. The six visible transition lines had Lorentzian absorption peak shapes with an intensity relation of 3:2:1:1:2:3.
A fit consisting of six separate Lorentzians added together was then applied to the data and from that fit the natural line width was determined in the range of 11.545 ± 1.89 neV and 18.48 ± 2.675 neV, which is larger than the accepted value of 4.7 neV [13], however is still an acceptable result since line broadening due to the many factors previously discussed will increase the theoretical value significantly.
Lande factors were calculated as being,

$$g_{1/2} = 0.178 \pm 0.006 \qquad \text{and} \qquad g_{3/2} = -0.102 \pm 0.003. \tag{18}$$

The ratio of these values was then taken as $g_{1/2}/g_{3/2} - 1.750 \pm 0.077$, which closely agrees with the ratio of the theoretical values of $g_{1/2}/g_{3/2} = -1.752 \pm 0.004$ [8].
Finally, an isomeric shift shift was calculated from the peak energy values to be $\Delta E_{iso} = [4.471 \pm 0.519]$ neV. A positive value was recorded however since the sign of the result depends on the which direction is arbitrarily chosen as positive, it is also possible to consider the value of $\Delta E_{iso} = [-4.471 \pm 0.519]$ neV. This negative isomer shift is caused by the smaller radius of ^{57}Fe in the excited state compared to the ground state.
We conclude that the Mößbauer spectrometer is able to provide extremely precise measurements which are consistent with literature values although not quite as precise. In order to achieve better results, more data could be recorded in order to provide a higher resolution. Newer and higher quality equipment could provide smaller sources of error and a digital interface could allow for a more precise tuning of the motor. A thorough calibration of the equipment could have been important to reducing the uncertainty before the experiment, and finally cooling the source and absorber could have provided narrower transition lines and therefore further reduced the uncertainty in our measurements.

References

[1] Mössbauer, Rudolf L.(1958): *Kernresonanzfluoreszenz von Gammastrahlung in Ir^{191}*, 2: 124-143.

[2] Evans, M J / Black, P J(1970): *Quadrupole splitting in sodium ferrocyanide*, 4: L81–L83.

[3] Evans, M J / Black, P J(1970): *The Voigt profile of Mossbauer transmission spectra*, 10: 2167–2177.

[4] Virtanen, Pauli u.a.(2020): *SciPy 1.0: Fundamental Algorithms for Scientific Computing in Python*261–272.

[5] Editors, Encyclopaedia (2016): *Hyperfine structure.* , Encyclopaedia Britannica inc.

[6] Lab, Tutors (1998): *K 221 Mößbauer effect.* , Universität Bonn.

[7] Perepelitsa, Dennis (2007): *Mossbauer Spectroscopy of 57 Fe.* .

[8] Physics, CalTech (2017): *The Mossbauer Effect: Hyperfine splitting.* , California Institute of Technology.

[9] Schatz, G. / Weidinger, A. (1997): *Nukleare Festkörperphysik.* , Teubner.

[10] Tatum, Jeremy (2020): *Combination of Profiles.* .

[11] Van Rossum, Guido / Drake, Fred L. (2009): *Python 3 Reference Manual*. Scotts Valley, CA, CreateSpace.

[12] Vértes, A. / Nagy, S. / Klencsár, Z. / Lovas, R.G. / Rösch, F. (2010): *Handbook of Nuclear Chemistry: Vol. 1: Basics of Nuclear Science; Vol. 2: Elements and*

Isotopes: Formation, Transformation, Distribution; Vol. 3: Chemical Applications of Nuclear Reactions and Radiation; Vol. 4: Radiochemistry and Radiopharmaceutical Chemistry in Life Sciences; Vol. 5: Instrumentation, Separation Techniques, Environmental Issues; Vol. 6: Nuclear Energy Production and Safety Issues.. , Springer US.

[13] Wang, Emily P. (2005): *Mossbauer Spectroscopy.* .

6 Appendix

The error propagation for an addition or subtraction is given by,

$$\delta Q = \sqrt{(\delta a)^2 + (\delta b)^2 + \cdots + (\delta c)^2 + (\delta x)^2 + (\delta y)^2 + \cdots + (\delta z)^2}. \tag{19}$$

Standard Gaussian error propagation is given by the general form of Summation in Quadrature,

$$\delta f\,(x, y, ...) = \sqrt{\left(\frac{\partial f}{\partial x}\delta x\right)^2 + \left(\frac{\partial f}{\partial y}\delta y\right)^2 + \cdots}. \tag{20}$$

Uncertainty in the counts of the Mößbauer spectrum were calculated according to,

$$\Delta N = \sqrt{\left(\sqrt{\left[\frac{N}{t/100}\right]^2}\right) + \left(\left[\frac{N/100}{(t/100)^2}\right]^2\right)}. \tag{21}$$